The 2010 IEEE/RSJ International Conference on
Intelligent Robots and Systems
October 18-22, 2010, Taipei, Taiwan

Design and Testing of a Controllable Miniature Jumping Robot

Jianguo Zhao, Ning Xi, Bingtuan Gao, Matt W. Mutka, and Li Xiao

Abstract— **Mobile sensors with jumping ability provide several advantages compared with the traditional wheeled sensors such as ability to move in rugged terrain. A controllable jumping robot for this purpose is described in this paper. The robot has dimension about** $9.5cm \times 9cm \times 3cm$ **and weighs** 54.1 **grams. It can perform the jumping process continuously. This paper focuses on the mechanisms to achieve such a continuous jumping ability, including the jumping mechanism, energy store and release mechanism, and self-righting mechanism. Detail implementation and experimental results are also given in this paper. It is shown that with a** 75° **takeoff angle, the robot can jump about** $20cm$ **in height.**

I. INTRODUCTION

Mobile sensor network consisting of multiple sensors with locomotion ability has various applications such as search and rescue, surveillance, and environmental monitoring. The most typical locomotion method in literature is wheeled sensors that can move continuously on land. Nevertheless, there is a trend to seek alternative locomotion methods such as jumping [1] and flying [2]. These methods possess several advantages compared with the wheeled locomotion. For example, the jumping sensors can overcome obstacles higher than themselves, which is impossible for wheeled ones. Therefore, jumping provides an ideal solution for rugged terrain locomotion. To achieve continuous jumping, the robot should be able to repeatedly perform the following motion sequences: first of all, it orients itself into the desired jumping direction, then the robot jumps with a certain takeoff angle, and finally, after landing on the ground, it can self-right from any possible landing posture and be ready for the next jump.

We have reported our initial research on jumping robot in [1], where the robot can only fulfill part of above jumping sequences: randomly throw the robot on the ground, the robot can self-right itself and jump one time. The aim of this paper is to present our new jumping robot which can achieve all the motion sequences except changing the jumping direction. The robot has a rectangular shape with dimension $9.5cm \times 9cm \times 3cm$ and weighs 54.1 grams. A picture of the robot is shown in Fig. 1.

Many robots with jumping ability have been designed in recent years. For robots to jump, there should be energy stored in the robot, and then a sudden release of the energy will make the robot thrust into the air. Grouping by energy storage method, existing jumping robots can be classified into three major categories: spring based design, pneumatic powered design, and combustion based design. In [3], a detail summary for existing jumping robots is given. Both the pneumatic and combustion based designs are complicated and cannot be implemented in small size. Since we are interested in miniature jumping robot, constrained by the size and weight limits, the most promising way is to use spring.

Fig. 1. The new jumping robot

For spring based design, a mechanism is used to transform the energy from the actuator into potential energy of the spring. After that, the stored energy is released to actuate a jumping mechanism or make the spring directly strike the ground, resulting the robot's jumping motion. For example, both the EPFL jumping robot [4] and the Grillo [5] use a cam to load torsional springs and then the springs release their energy through a four bar mechanism. The Mini-Whegs™ uses a slip-gear mechanism to load an extension coil spring, which again actuates a four bar mechanism after the load process [6]. The second generation JPL hopper uses a coil spring placed at the center of a geared six bar mechanism to create a nonlinear force-displacement curve which has a better performance than a four bar mechanism [7]. The scout uses cable winded along a capstan to load a bending plate spring and achieves jumping by directly punching the ground [8]. Similarly, the Microbot uses elastomer actuators and cables to load two symmetrical bending springs which directly contact the ground [9]. Encircled by several metal semi-circular hoops, the Jollbot has a spherical structure which can change its shape by the variable length crank mechanism inside the sphere, whose shape deformation can cause the robot to jump [3].

Unlike above robots designed exclusively for locomotion in rugged terrain, we want to design a jumping robot for

This work is supported by the National Science Foundation under Grant NO. CNS-0721441

Jianguo Zhao, Ning Xi, and Bingtuan Gao are with Department of Electrical and Computer Engineering, Michigan State University, MI, 48824, USA. zhaojia1@msu.edu, xin@egr.msu.edu, carlgao@msu.edu

Matt W. Mutka and Li Xiao are with the Department of Computer Science and Engineering, Michigan State University, East Lansing, MI, 48824, USA. {mutka, lxiao}@cse.msu.edu

mobile sensor networks. This application requires the robot to be low cost, miniature, and lightweight. All the existing miniature jumping robots are based on spring. However, most of such robots cannot jump very high. For example, the jumping heights of Grillo [5], Mini-Whegs^{TM} [6], scout [8], or Jollbot [3] are all below $0.35m$. An exception is the EPFL jumping robot which can jump $1.38m$ with 7 gram weight, but adding a cage for self-righting with a total weight 14 grams can reduce the jumping height to $0.62m$ [4]. In sensor network application, the sensor nodes should be able to carry various sensors for data acquisition. Therefore, the challenge is to design a new jumping robot so that it can jump high with considerable payloads.

To realize the jumping motion sequences discussed above, the robot should have three major components, which are elaborated and analyzed in section II, III, and IV respectively in the rest of paper. After that, all the mechanisms as a whole are illustrated and the theoretical jumping height is derived. Finally, the experimental results and conclusions are given.

II. Jumping Mechanism

A. Mechanism Synthesis

In nature, most animals with jumping ability use the same principle to jump. At first, their feet exert forces on the ground, and the reaction force from the ground makes their body accelerate upward. After the body velocity reaches a threshold value, it will bring the foot to leave the ground and jump [10]. The jumping mechanism should also provide the same function. To accelerate the robot body using springs, various mechanisms can be used. The simplest way is directly using the spring force such as our previous robot [1], the scout [8], and the Microbot [9]. This method, however, may lead to premature takeoff from the ground before the energy stored in the spring is totally released. Another approach is to use a spring actuated four bar mechanism such as the EPFL jumping robot [4], the Grillo [5], and the Mini-Whegs^{TM} [6].

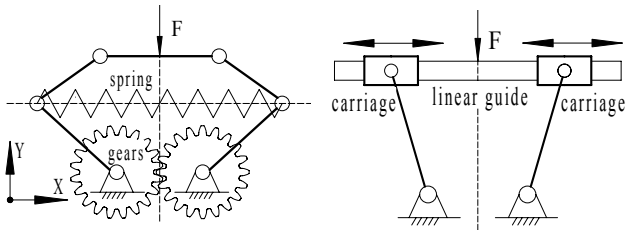

(a) 2-RRR mechanism (b) 2-RRP mechanism

Fig. 2. Jumping mechanism

Aside from above two methods, a geared six bar mechanism shown in Fig. 2(a) is used for jumping in the JPL hopper [7]. The mechanism consists of two identical rotational-rotational-rotational limbs, connecting by an extension spring. This mechanism, also called geared 2-RRR mechanism, in fact creates a nonlinear spring (the relation between force F and vertical displacement along Y axis is nonlinear) which is suitable for body acceleration. Moreover, its symmetrical structure facilitates the spring load process: we can exert a vertical force F in the middle of top bar to store energy in the spring. Therefore, we use this idea for our new jumping robot. However, for this mechanism, during the acceleration period, the traveling length along Y axis is very long, which is not suitable for our application because of size limit. To reduce the vertical traveling length, we propose a 2-RRP mechanism as shown in Fig. 2(b) which has two identical rotational-rotational-prismatic limbs. In this mechanism, two carriages move along a linear guide, resulting the vertical displacement.

Both of the 2-RRR and 2-RRP mechanisms have three degree-of-freedom (DOF), which can be easily verified by the Kutzbach-Grübler mobility formula. To accelerate the body, only one DOF is needed, while the other two DOF should be constrained. We can use two gears as what the JPL hopper does, but the gears serve as resistance during the acceleration and will cause energy loss. Another two methods exist as shown in Fig. 3. The first one, shown in Fig. 3(a), is to use a parallelogram to make the linear guide always parallel to the base. The second method, shown in Fig. 3(b), is to use two rods which are fixed to the base and go through the linear guide so that the linear guide can only move in vertical direction. Since the first one involves many rotational joints, we choose the second method for our design.

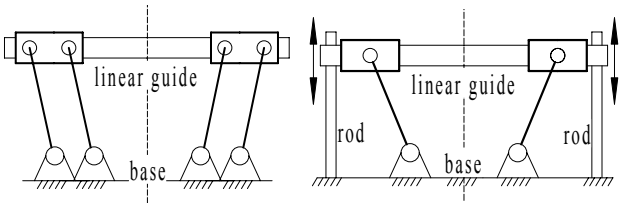

(a) With parallelogram (b) With two rods

Fig. 3. Different methods to constrain two degree-of-freedoms

B. Different Spring Actuation Methods

Having chosen the jumping mechanism shown in Fig. 3(b), we still face multiple choices of different spring actuation methods, i.e., we can use different springs which may furthermore be placed at different places. The best choice should be the one which needs minimum force to load the springs so that the final stored energy is the same. Smaller spring load force can be provided by lighter motors, which can reduce both the weight and cost for the robot. Therefore, we need to compare the maximum spring load force with the same energy stored in the springs.

As stated in the introduction section, most spring based jumping robots cannot jump above $0.35m$. Therefore, we want our robot to jump $h = 0.35m$. This height can be used to estimate the required energy stored in the spring. According to our previous work [1], all the mechanisms for jumping robot can be divided into two parts: upper mass and lower mass, and the vertical jumping height is give as:

$$h = \frac{m_2 E_0}{(m_1 + m_2)^2 g}$$

where m_1 and m_2 are the mass for the lower mass and upper mass, respectively. In our previous design, we have $m_1 = 19.3g$ and $m_2 = 21.8g$ [1]. For the new robot, we expect $m_1 = 20g$ and $m_2 = 40g$ (m_2 is larger since we are adding an autonomous load and a self-righting mechanism to the upper mass). Using the above formula we can obtain $E_0 = 0.31J$. To leave some margin, let E_0 be $0.35J$.

Although there exist many different alternatives, only two typical different spring actuation methods, shown in Fig. 4, will be discussed. Note that we omit the two rods for clarity in the figure. To get the maximum spring load force for each case, we try to obtain the function relating the spring load force F with the vertical position y. The zero position of y is at the middle of the two rotational joints of the base. Let the distance between two rotation joints at the base be $l_1 = 15mm$ and the length of the rotational link be $l_2 = 35mm$. The distance between the two carriages satisfies $l_{3min} < l_3 < l_{3max}$. We let $l_{3min} = 35mm$ since another mechanism will be placed between the carriages; we let $l_{3max} = 80mm$ since the length of linear guide is $94mm$. Under these conditions, the vertical displacement satisfies $13.0mm < y < 33.5mm$, which means the vertical traveling distance for the linear guide will be $d = 20.5mm$. We also assume the frictional force between the carriages and the linear guide is negligible.

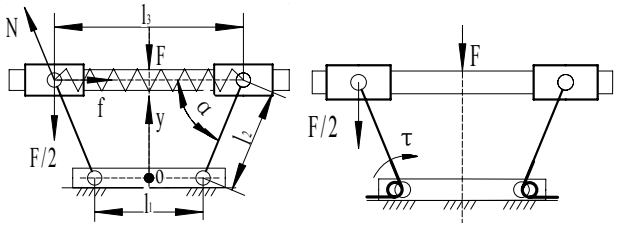

(a) Case one (b) Case two

Fig. 4. Different spring actuation methods

1) Case One: An extension spring is placed between the two carriages. The static force analysis for the left carriage is shown in Fig. 4(a), where f is the spring force, $F/2$ is half of the load force, and N is the reaction force from the rotational link with direction along the link. Suppose the initial length of the spring is $l_0 = l_{3min}$, from the static force balance, we have:

$$F = 4ky + \frac{2ky(l_1 - l_{3min})}{\sqrt{l_2^2 - y^2}} \tag{1}$$

where k is the spring constant obtained from:

$$\frac{1}{2}k(l_{3max} - l_{3min})^2 = E_0$$

2) Case Two: In this case, two torsional springs with deflection angle 90° are placed at the two rotational joints at the base as shown in Fig. 4(b). The left rotational link is subject to a force equal to half the spring load force and a moment τ from the torsional spring. From the moment balance for the rotational link, we have:

$$F = \frac{k\pi - 2k\arcsin(y/l_2)}{\sqrt{l_2^2 - y^2}} \tag{2}$$

where k is the spring constant derived from:

$$k(\frac{\pi}{2} - \alpha_{min})^2 - k(\frac{\pi}{2} - \alpha_{max})^2 = E_0$$

where $\alpha_{min} = 0.3803$ and $\alpha_{max} = 1.2810$ correspond to the value of $\alpha = \arccos\frac{l_3 - l_1}{2l_2}$ when $l_3 = l_{3max}$ and $l_3 = l_{3min}$, respectively.

With Eqs. (1) and (2), we can plot the spring load force versus vertical displacement as shown in Fig. 5. In the figure, the solid line is for case one, while the dashed line is for case two. From the figure, we can see the second case has a smaller peak force, for which a smaller motor can accomplish the load process.

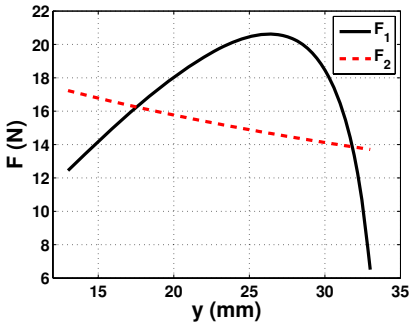

Fig. 5. Spring load force versus vertical displacement

In practice, we use four torsional springs, two at each rotation joint, for easy implementation. Then the desired spring constant can be derived as $117.6Nmm/rad$ from the required energy $0.35J$. The torsional spring closest to the desired value we can find is $154.1Nmm/rad$. For this spring, we can get the peak load force as $F_p = 22.6N$, which will be used later to derive the speed reduction for the load process.

III. Energy Store and Release Mechanism

With the jumping mechanism discussed in previous section, we need another mechanism to store energy in the spring and release it when necessary. This includes three steps: load the spring at first: store energy in the spring, then hold the spring: keep the energy, and finally release the spring: free the energy. In this section, the detail design for these three parts will be discussed.

A. Spring Load Mechanism

For spring load, we use a mini DC motor to drag a cable connecting the linear guide and the base so that a resulting load force can pull the linear guide to get close to the base. The idea is shown in Fig. 6(a). To make the load process stable, the cable is placed symmetrically at two sides of linear guide, with the right end fixed to the linear guide, and the left end attached to the DC motor actuated capstan. Two pulleys

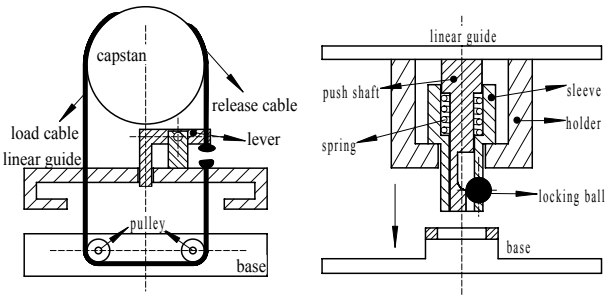

(a) Load and release mechanism (b) Hold mechanism

Fig. 6. Spring load, hold, and release mechanism

are used at the base to guide the cable, which can also reduce load force by half for the motor.

As discussed in previous section, the peak load force is $F_p = 22.6N$. As a result of the two pulleys, the peak force is $F_p' = 11.3N$. With design consideration for the self-righting mechanism which will be discussed later, we want the capstan to rotate one cycle to load the spring. As a result, the capstan should have a perimeter twice the vertical traveling distance, from which we can obtain the radius of the capstan as $r = d/\pi = 6.5mm$. Thus we need a torque $F_p' r = 73.5Nmm$ to load the spring. The motor (GH810136V3 from Gizmo's zone) we are using has a stall torque $250gcm = 25Nmm$ [11]. To leave some margin to overcome friction in the gear system, we use two stage speed reduction with gear ratios $9/28$ and $10/30$. A motor gear (GM0.5-09-14), a compound gear (GC0.5-10/28-20), and a spur gear (GS0.5-30-29) from the same company are used.

B. Spring Hold Mechanism

For spring hold, we use a quick release detent ball mechanism as shown in Fig. 6(b). The holder is rigidly connected to the linear guide and holds all the mechanism. The sleeve can move up and down in the holder. There is a hole in the sleeve which has a diameter slightly smaller than the locking ball, making most part of the ball can come out but not come out entirely. The push shaft contacts the linear guide by the compression spring and can move up and down in the sleeve. The push shaft has a groove, which can accommodate the locking ball. A round hole in the base with a little larger diameter than the sleeve can make the sleeve get across when the ball is contained in the groove of push shaft. The hold process, as shown in Fig. 7, has three steps:

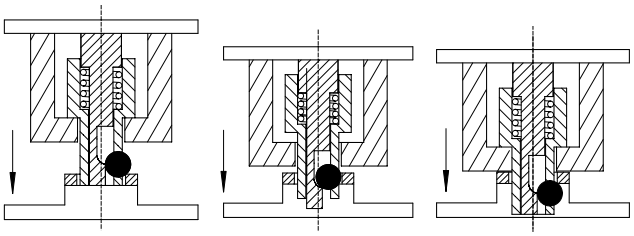

(a) Step one (b) Step two (c) Step three

Fig. 7. Spring load and hold process

1) During the load process, the linear guide together with the hold mechanism is pushed close to the base. Once the locking ball contacts the round hole at the base, the sleeve will stop moving because of the reaction force from the base, but the push shaft will continue to move down since it directly contacts the linear guide.
2) Along with the downward movement of the push shaft, the locking ball will move inside until it is contained in the groove. Then the sleeve can also move down.
3) After the hole on the sleeve passes the base hole, the sleeve will move down further because of the spring force, pushing the locking ball out again. At this time, if the load force is removed, the locking ball can hold the mechanism at current position.

C. Spring Release Mechanism

To release the stored energy, we use a mechanism to strike the push shaft. With the shaft moving down, the locking ball will retract to the groove again, and the energy will be thus released. The strike mechanism is a lever with one end contacting the push shaft and the other end dragged by the release cable as shown in Fig. 6(a).

Note that the load and release processes are actuated by a single motor. The capstan in Fig. 6(a) has two channels, one for load cable and the other for release cable. When the motor runs clockwise (CW), the load cable contracts, while the release cable extends. After the robot is locked by the hold mechanism, the motor runs counterclockwise (CCW). In this case, the load cable extends, while the release cable contracts. When the load cable extends to initial unloaded state, the release cable is about to drag the lever and release the stored energy. In addition, the release force only depends on a small constant compression spring in the sleeve. As a result, the release force is much smaller than the load force, and we can easily release the energy with the same motor.

IV. Self-righting Mechanism

The landing posture for jumping robot is highly unpredictable; therefore, it is critical to have a self-righting mechanism so that the robot can stand up. Usually, the robot is built as a spherical shape and achieves self-righting by changing the robot's center of gravity [1], [3], [4]. This method, however, is passive, which cannot always ensure proper self-righting. We propose to use an active method. Instead of spherical shape, the robot has a rectangular shape with two faces much larger than the other four faces. Under this condition, the robot will contact ground with one of the two largest surfaces most of the time because the other four surfaces are quite small, which is not stable for the robot to lie on the ground. Thus we only need to design a mechanism to recover from the case for the two largest surfaces.

An illustration of the self-righting is shown in Fig. 8, where the red parts are self-righting mechanism. Two legs, parallel to each side of the two largest surfaces, can rotate in opposite directions. When they rotate simultaneously, the robot can stand up no matter which largest surface the robot contacts the ground. Suppose the takeoff angle for the robot

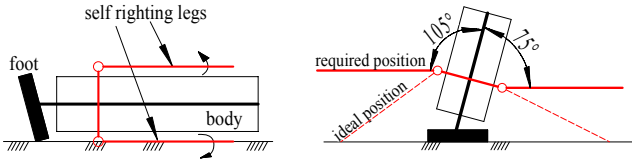

(a) Before self-right (b) After self-right

Fig. 8. Illustration of active self-righting

is 75° and the fully unfold status for the mechanism is when both legs are parallel to the ground, which is shown as the required position in Fig. 8(b). Then the rotation angles for the two legs should be 75° and 105°, respectively.

To fulfill above goal with a single motor, a symmetrical mechanism shown in Fig. 9(a) for flapping wing flying is a good candidate [12]. In this case, a slider-crank mechanism actuates two symmetrical rotational-prismatic-rotational chains. However, this mechanism is quite complicated, and the symmetrical structure makes the rotation range for two legs be the same. But the robot needs different ranges (75° and 105°). Therefore, we propose the mechanism shown in Fig. 9(b), which consists of six rotational joints plus one prismatic joint. When the upper rotational joint rotates CCW, the left leg will rotate CCW and the right leg will rotate CW.

Suppose the angles between left leg and vertical line, right leg and vertical line, AB and vertical line are α, β and θ respectively as shown in Fig. 9(b). To achieve the self-righting purpose, we want $\alpha_{max} > 75°$ and $\beta_{max} > 105°$ as the required condition. Note that in the ideal case, the two legs should be at the ideal position as shown in Fig. 8(b). In this case, the maximum angles for both α and β are larger than the required case. Therefore, to get the best self-righting result, an optimal design should be performed to maximize both α and β. However, as our initial design, it suffices to use trial and error method in ADAMS to obtain the design results satisfying the required condition.

In the coordinate system shown in Fig. 9(b) with origin at the middle of ED and X direction along $\overrightarrow{ED}$, one good design has the following parameters: $A = (0, 27.14)$, $D = (5.5, 0)$, $E = (-5.5, 0)$, $|AB| = 6$, $|BC| = 27.18$, and $|CD| = 7.21$ (the unit is mm). The angular displacements for α and β when θ runs from 0 to 2π are shown in Fig. 10. The maximum

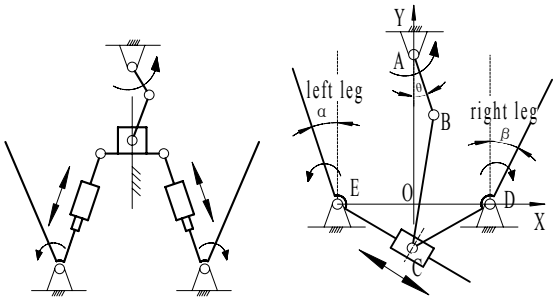

(a) Symmetrical mechanism (b) Unsymmetrical mechanism

Fig. 9. Possible self-righting mechanisms

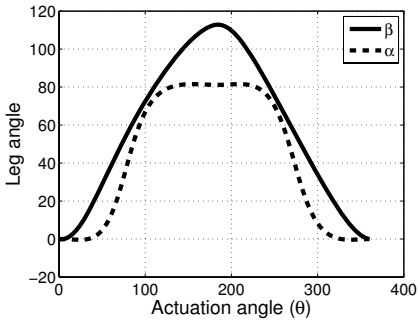

Fig. 10. Leg angle curve with respect to the actuation angle

angle is 112.9° for α and 81.9° for β, which are both larger than the required angles.

V. Implementation and Experimental Results

The exploded 3D model of the robot is shown in Fig. 11. All the mechanisms discussed above are encircled by dashed lines. Note that the load cable, release cable, and most of the connection components are not shown for clear view. We have discussed how to use a single motor to both load and release spring energy. In fact, all the mechanisms are actuated by a single motor. The self-righting mechanism is connected to the same shaft for load and release by a one-way bearing. Due to such a bearing, the self-righting mechanism can only be actuated when the motor runs CCW.

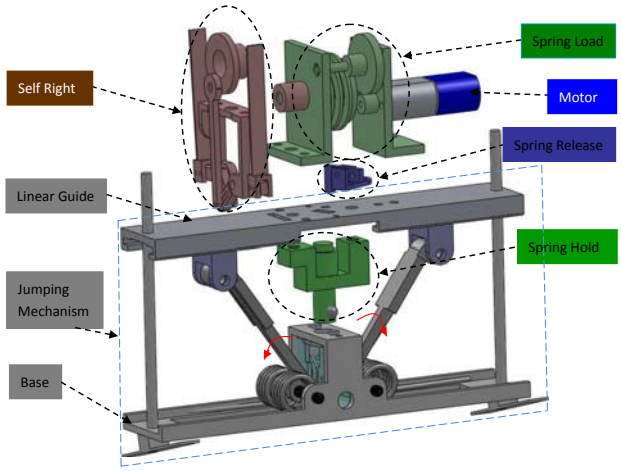

Fig. 11. Exploded 3D model of the jumping robot

Using above three major mechanisms, the continuous jumping can be achieved. First of all, the motor rotates CW and loads the spring to store energy until the locking ball is able to lock the robot. Secondly, the motor runs CCW to extend the load cables, while at the same time the self-righting mechanism makes the robot stand up. Thirdly, after the stand up, a little CCW rotation of the motor will cause the release mechanism to free the stored energy. Finally, the robot jumps into the air, and lands on the ground. Then the robot can repeat above motion continuously.

For the mechanical part of the robot, various materials with low density but good mechanical properties are used to reduce robot weight, including Acetal, Nylon, PEEK, Derlin, carbon fiber, aluminum, and Polycarbonate. The aluminum linear guide is modified from the DryLin®N Low Profile Linear Guide System of igus [13]. There are lots of rotational parts in the robot. For the parts where rotation is frequent such as in the speed reduction mechanism, we use miniature bearings. For the less frequent rotation parts such as in the self-righting mechanism, a pin-hole structure is used.

Since the initial objective is focused on the mechanical part, for the control part, we simply adopt a wireless remote control method. Two Xbees from Digi, one attached to the robot and the other to the computer, are used to establish the wireless link. One Atmega 328p microcontroller is used to receive the command from Xbee and control the motor's rotation direction through an H-bridge IC. The total energy for the robot is provided by a 100mAh LiPo battery.

The total weight for the robot is 54.1g. To derive the theoretical jumping height, we divide the robot into upper mass and lower mass. The lower mass, with a weight $m_1 = 16.5g$, includes base: 5.3g, four springs: 5.2g, rotational link parts: 4.2g, two feet and rods: 1.8g. Note that the weight for base including the pulleys for spring load. The upper mass, with a weight $m_2 = 37.6g$, includes linear guide: 10.2g, motor: 3.9g, spring load: 5.9g, self-righting: 3.3g, spring hold: 1.8g, spring release: 0.3g, control parts: 10.5g, and other screws and nuts: 1.7g.

Fig. 12. Experimental jumping height

Given the robot's takeoff angle $\gamma = 75^\circ$ and weights for lower and upper mass, we can calculate the theoretical jumping height. From the tilted model in [1], the height is given as:

$$h = \frac{m_2 E_0 \sin^2 \gamma}{(m_1 + m_2)^2 g} = 52.8\,cm$$

where $E_0 = 2k(\frac{\pi}{2} - \alpha_{min})^2 - 2k(\frac{\pi}{2} - \alpha_{max})^2$ is the initial energy stored in the four springs.

The experiment is performed on an desk, and the performance is obtained from a video that records the jumping procedure. As shown in Fig. 12, an individual frame from a video, the height is about $20cm$, which is much smaller than the theoretical height. The reason is that in theoretical analysis, we don't consider the energy loss resulting from the friction between the carriage and linear guide and the friction between the linear guides and two rods.

In addition to the jumping height, the self-righting mechanism can successfully make the robot stand up provided the leg length is long enough. One problem is the mechanism depends on the CCW rotation of the motor, which cannot guarantee the legs return to the initial position. In this case, after a few cycles, the whole motion sequence can be wrong. Possible solution, instead of using the motor's rotation, can use the downward motion of the linear guide to perform self-recovery.

VI. Conclusion

A new controllable jumping robot for mobile sensor network is presented in this paper. Three major mechanisms, including jumping mechanism, spring load, hold, and release mechanism, and self-righting mechanism, endow the robot with continuous jumping ability. All the mechanisms are actuated by a single motor. The experimental results show poorer performance than theoretical results, which is because of the simplification in theoretical analysis. Nevertheless, the mechanisms for the jumping robot in this paper may provide valuable references for nontraditional robot design. Further optimization of the mechanism will be performed to achieve the goal of $35cm$ jumping height.

References

[1] J. G. Zhao, R. G. Yang, N. Xi, B. T. Gao, X. G. Fan, M. Mutka, and L. Xiao, "Development of a self-stabilization miniature jumping robot," *IEEE/RSJ Int. Conf. Intelligent Robots And Systems*, St. Louis, MO, 2009, pp. 2217-2222.

[2] A. Purohit and P. Zhang. 2009. "SensorFly: a controlled-mobile aerial sensor network," *Proceedings of the 7th ACM Conference on Embedded Networked Sensor Systems* (Berkeley, California, November 04 - 06, 2009). SenSys '09. ACM, New York, NY, pp. 327-328.

[3] R. Armour, K. Paskins, A. Bowyer, J. Vincent, and W. Megill, "Jumping robots: a biomimetic solution to locomotion across rough terrain," *Bioinspiration and Biomimetics Journal*, vol. 2, no. 3, pp. 65-82, 2007.

[4] M. Kovac, M. Schlegel, J. Zufferey, and D. Floreano, "Steerable miniature jumping robot," *Autonomous Robots*, vol. 28, no. 3, pp. 295-306, 2010.

[5] U. Scarfogliero, C. Stefanini, and P. Dario, "Design and Development of the Long-Jumping Grillo Mini Robot," *International Conference on Robotics and Automation*, Roma, Italy, 2007, pp. 467-472.

[6] B. G. A. Lambrecht, A. D. Horchler, and R. D. Quinn, "A small, insect inspired robot that runs and jumps," *International Conference on Robotics and Automation*, Barcelona, Spain, 2005, pp. 1240-1245.

[7] J. Burdick and P. Fiorini, "Minimalist Jumping Robots for Celestial Exploration," *International Journal of Robotics Research*, vol. 22, no. 7, pp. 653-674, 2003.

[8] S. A. Stoeter and N. Papanikolopoulos, "Kinematic Motion Model for Jumping Scout Robots," *IEEE Transactions on Robotics and Automation*, vol. 22, no. 2, pp. 398-403, 2006.

[9] S. Dubowsky, S. Kesner, J. Plante, and P. Boston, "Hopping mobility concept for search and rescue robots," *Industrial Robot: An International Journal*, vol. 35, no. 3, pp. 238-245, 2008.

[10] R. M. Alexander, *Principles of Animal Locomotion,* Princeton University Press, 2003.

[11] Gizmo's zone, Website: http://www.gizmoszone.com

[12] C. Dileo and X. Y. Deng, "Design of and Experiments on a Dragonfly-Inspired Robot," Advanced Robotics, vol. 23, no. 7-8, pp. 1003-1021, 2009.

[13] Igus, Linear guide system, Website: http://www.igus.com/show_dn.asp